Mean Monthly Diurnal Cycles Observed with PRE-STORM Surface Data

PAUL M. MARKOWSKI

School of Meteorology, University of Oklahoma, Norman, Oklahoma

DAVID J. STENSRUD

NOAA/ERL/National Severe Storms Laboratory, Norman, Oklahoma

(Manuscript received 28 May 1997, in final form 1 January 1998)

ABSTRACT

Data from 84 surface mesonetwork stations deployed across Oklahoma and Kansas are used to calculate monthly mean diurnal cycles at each mesonetwork site during May and June of 1985 during the Preliminary Regional Experiment for Stormscale Operational and Research Meteorology (PRE-STORM). The horizontal variations in mean monthly temperatures and specific humidities are large, even though this experimental domain covers only a portion of each state. Landscape differences cause much of this variation, with the harvesting of winter wheat over a large region of Oklahoma in late May being one of the more clear factors influencing the surface layer cycles.

A subjective classification of the mean monthly diurnal cycles shows that the type of diurnal cycle changes as the vegetation changes. However, this relationship is strongly modified by the effects of convection. Results suggest that the mean diurnal cycles include the effects of convective downdrafts, indicating that the interaction of convection with the atmospheric surface layer is an important process even on monthly timescales. This is important to consider for those trying to evaluate regional climate simulations.

1. Introduction

The planetary boundary layer (PBL) plays a critical role in the development of mesoscale weather systems. The large fluxes of heat, moisture, and momentum that occur in this layer often can set limits on the types of weather phenomena that can be produced on a given day. While the surface radiation balance drives the boundary layer evolution, characteristics of the landscape determine the relative amounts of sensible and latent heat flux into the boundary layer.

During the past decade the importance of landscape characteristics, such as vegetation, soil moisture, surface roughness, and soil type, has been shown clearly through the use of numerical models that attempt to realistically simulate the boundary layer over mesoscale-sized regions. Several numerical simulations suggest that sea-breeze-type circulations can develop near boundaries between wet and dry land regions (Anthes 1984; Ookouchi et al. 1984; Mahfouf et al. 1987; Segal et al. 1988; Avissar and Liu 1996). Chang and Wetzel (1991) further illustrate that spatial variations of vegetation and soil moisture influence surface baroclinic structures through differential heating, and that strong gradients in landscape characteristics are crucial to simulating the proper placement and intensity of surface discontinuities.

Differential surface heating due to varying landscape characteristics also has been found to be important to severe storm environments. Lee troughing was intensified owing to differential heating in the simulations of Benjamin and Carlson (1986), which, in turn, increased the low-level moisture flux toward the region of initial storm development. The strength and depth of elevated mixed layers, which are important to convective inhibition (Carlson and Ludlam 1968; Carlson et al. 1980, Carlson et al. 1983; Graziano and Carlson 1987; Stensrud 1993), the creation of convective available potential energy (Doswell et al. 1985), and the development and evolution of the dryline (Rhea 1966), are influenced by differential heating and evaporation due to varying landscape characteristics (Benjamin and Carlson 1986; Lanicci et al. 1987; Lakhtakia and Warner 1987). The dryline, often a focus of convective initiation, also is sensitive to landscape variations (Ziegler et al. 1995). The connection between differential heating and evaporation and the production of precipitation is shown clearly by Lakhtakia and Warner (1987) and Lanicci et al. (1987), further underscoring the importance of landscape characteristics to precipitating mesoscale systems.

The more obvious role of landscape characteristics is in the determination of boundary layer temperature and

Corresponding author address: Dr. David J. Stensrud, National Severe Storms Laboratory, 1313 Halley Circle, Norman, OK 73069. E-mail: David.Stensrud@nssl.noaa.gov

moisture structures. Diak et al. (1986) show that the accuracies of daytime surface temperature predictions are sensitive to small changes in moisture availability in dry regions. Convective cloud development also is influenced by the landscape. In a study of a mesoscale-sized area over Oklahoma, Rabin et al. (1990) documented that clouds first formed over a region of wheat stubble where the ground temperature was 1°–2°C warmer than the surrounding regions. In contrast, cloud formation was found to be suppressed downwind of lakes and heavily forested areas. Areas of irrigated crops also influence the lower PBL as shown by both observations and modeling (Segal et al. 1989).

A different approach to determining the influence of surface processes upon boundary layer evolution involves the use of conserved variable diagrams (Betts 1982, 1984). Betts (1982) shows that the conserved variable approach allows for the interpretion of irreversible processes acting upon a parcel as movement of the parcel saturation point in known directions on a conserved variable diagram. Betts (1984, 1992) expands this technique to examine the PBL-sensible and latent heat budgets, where the surface and inversion level fluxes are denoted as vectors on a conserved variable diagram. Using this technique, Betts et al. (1992) show the high correlation between the trends seen in surface data and those in the well-mixed PBL. Betts and Ball (1995) further show the significant effects of soil moisture on the diurnal cycle from surface data averaged over a six-month period. They believe that surface data averaged over such a long time period can be used to test and develop coupled land surface and boundary layer parameterization schemes for global models.

The goal of this paper is to explore the amount of information on physical processes that can be extracted from the monthly mean diurnal cycles calculated from the 84 surface mesonetwork stations deployed across much of Kansas and Oklahoma during May and June of 1985 in support of the Preliminary Regional Experiment for Stormscale Operational and Research Meteorology (PRE-STORM) (Cunning 1986). This monthly averaging period is much less than the six-month average used by Betts and Ball (1995), and thus may illustrate the importance of processes with shorter temporal scales to PBL evolution. In addition, since the monthly average diurnal cycle is calculated at each mesonetwork station, the data may also suggest the relative importance of the horizontal changes in landscape (e.g., vegetation type, soil type, vegetation coverage) that occur across the PRE-STORM domain to PBL evolution.

This research is aimed at helping to define the processes needed to represent the mean monthly boundary layer evolution over land, and that must then be parameterized in numerical weather prediction models in order to successfully model regional climate and produce seasonal forecasts. Betts et al. (1993) compared an observed diurnal cycle with one produced by the European Centre model and identified many errors in the model

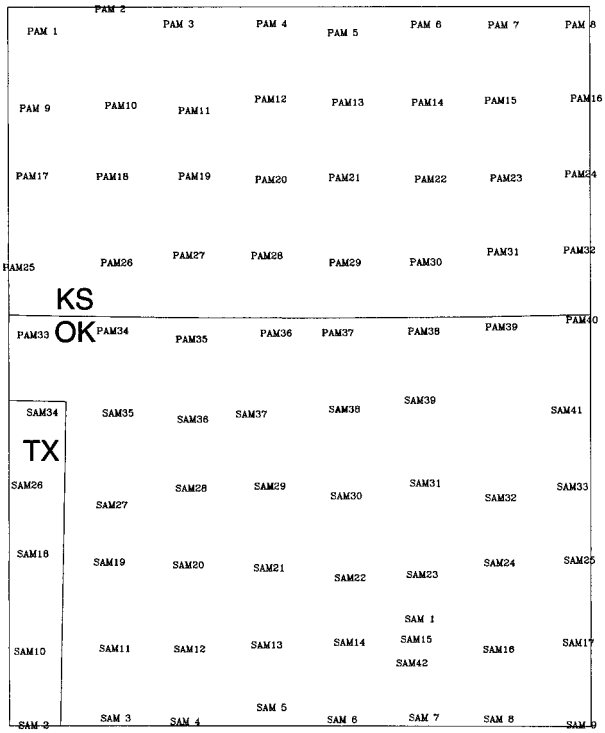

FIG. 1. Locations of the mesonetwork stations during the PRE-STORM experiment. Stations are either the NSSL Surface Automated Mesonet (SAM) stations or the NCAR Portable Automated Mesonet (PAM) stations and are denoted by SAMXX or PAMXX, respectively, where XX is the station number.

parameterizations. It is hoped that this study may provide the impetus for further comparisons between models and surface observations using the conserved variable approach.

The data used in this study are discussed briefly in section 2, followed by an examination of the effects of landscape in section 3. A classification of the main types of diurnal cycles is conducted in section 4. A calculation of the surface Bowen ratios is presented in section 5, followed by conclusions in section 6.

2. Data

During the 1985 PRE-STORM experiment, 84 automated surface mesonetwork stations were deployed across much of Kansas and Oklahoma with an average spacing of approximately 50 km (Fig. 1). These stations measured 5-min average values of temperature, wet bulb temperature, wind, and pressure beginning 1 May 1985 and ending 27 June 1985, and, in addition, provided 5-min maximum wind gusts and 5-min accumulated precipitation. The southern half of the mesonetwork stations were comprised of the National Severe Storms Laboratory (NSSL) Surface Automated Mesonet (SAM) stations, while the northern half of the mesonetwork stations were composed of the National Center for Atmospheric Research (NCAR) Portable Automated Me-

sonet (PAM) stations. The data were calibrated and adjustments made to the dataset during archival. Although 5-min data are available, the mesonetwork data taken on the hour only are used to calculate the monthly mean diurnal cycles of temperature (T), potential temperture (θ), specific humidity (q), and surface pressure. A five-point median filter is used with the 5-min data to remove any small-scale noise from the calculations.

Two approaches are used to examine the monthly mean diurnal cycles. The first approach objectively analyzes the mean station data to a regular grid using a Cressman (1959) weighting function with a 90-km influence radius in order to view the horizontal variations across the mesonetwork. The second approach plots the mean data from an individual surface station on a conserved variable diagram. Results indicate that both approaches must be used to obtain a better understanding of the physical processes controlling the mean diurnal cycles.

The use of conserved variables greatly simplifies examinations of the processes that drive boundary layer evolution (Lilly 1968; Betts 1973, 1975). One approach is based upon the use of a saturation point (SP) framework (Betts 1982, 1984, 1985). The SP of an unsaturated air parcel is found by lifting the parcel dry-adiabatically until it just becomes saturated. Any two combinations of the values of potential temperature, specific humidity, and pressure at the saturation level (θ^*, q^*, p^*) uniquely determine the thermodynamic properties of this parcel. Since the atmospheric surface layer is generally unsaturated (except when fog is present), and θ and q are conserved in a dry-adiabatic process, the surface layer values of θ and q are equal to the saturation level values (θ^*, q^*).

The thermodynamic properties of the surface layer and the lower boundary layer can be idealized as two air parcels originating at different pressure levels and with different values of θ and q (Betts 1984), where the surface layer typically is warmer and moister than the boundary layer during the daytime. As these two parcels mix isobarically, the SP of the mixture lies on a mixing line connecting the SPs of the two air parcels (Betts 1982). This framework allows boundary layer evolution to be viewed as being driven by three mixing processes (Betts 1984, 1992): the first is mixing between the surface layer and the lower boundary layer (representing surface fluxes), the second is mixing within the boundary layer itself, and the third is mixing between the upper boundary layer and the free atmosphere above (representing entrainment fluxes). If the boundary layer is well mixed, then this idealization reduces to mixing processes at just the surface and the inversion. Mixing with the surface layer produces warming and moistening, while mixing with the free atmosphere produces warming and drying. While this conserved variable approach is an idealization of PBL processes, it is a good framework from which to examine the surface mesonetwork data. We begin this examination by viewing the horizontal variability seen in the mesonetwork data.

3. Horizontal variations

The mean values of T and q at the time of maximum temperature (2100 UTC) for both May and June (Fig. 2) indicate significant gradients across the PRE-STORM mesonetwork, with consistently higher values of q to the east and southeast. The east–west gradient in q is related in part to the change in vegetation that occurs, with forests being found in eastern Oklahoma and prairie being found in western Oklahoma. Studies that characterize the spatial patterns of rainfall during the warm season indicate that a boundary between rainfall regimes stretches north to south across central Oklahoma for periods between 3 and 15 days (Richman and Lamb 1985, 1987, 1990). For 30-day periods, this longitudinal separation of rainfall regimes is no longer apparent and instead an east–west boundary is found that lies near the Kansas–Oklahoma border (Richman and Lamb 1990). Rainfall totals from the PRE-STORM mesonetwork stations for May and June agree qualitatively with these results, showing higher rainfall totals in the eastern parts of Kansas and Oklahoma, with overall higher rainfall totals in Kansas as compared to Oklahoma (Fig. 3). Thus, part of the east–west gradient in q values also likely is related to the rainfall distribution during the month.

Examination of the T fields indicates a distinct axis of higher T values in western Oklahoma that extends into southern Kansas during both months (Figs. 2a,c). This ridge likely is caused by the variability of the landscape, since the growing season in Oklahoma typically begins in March and April (Loveland et al. 1995). Rabin et al. (1990) found a zone of higher surface temperatures in western Oklahoma that accompanied the harvesting of winter wheat during late May and early June of 1988. The placement of the region of higher surface temperatures found by Rabin et al. (1990) nearly overlaps that indicated in the monthly average T values from the PRE-STORM mesonetwork. The land cover data from Loveland et al. (1995) clearly shows that the region of wheat farming in Oklahoma corresponds well with the zone of higher surface temperatures and lower mixing ratios (cf. Figs. 2 and 4). However, wheat harvesting typically is not done until later in May, whereas the monthly mean temperature field clearly indicates warmer temperatures in the region of winter wheat. To investigate the cause of the temperature ridge, the mesonetwork data is further subdivided into 15-day intervals. This analysis shows that the zone of warmer temperatures did not appear until the last half of May and persisted throughout June (Fig. 5). This dramatic increase in temperature during late May strongly suggests that the maturing and harvesting of winter wheat is the cause of this temperature anomaly and illustrates a possible effect of human beings on climate variability on a seasonal basis.

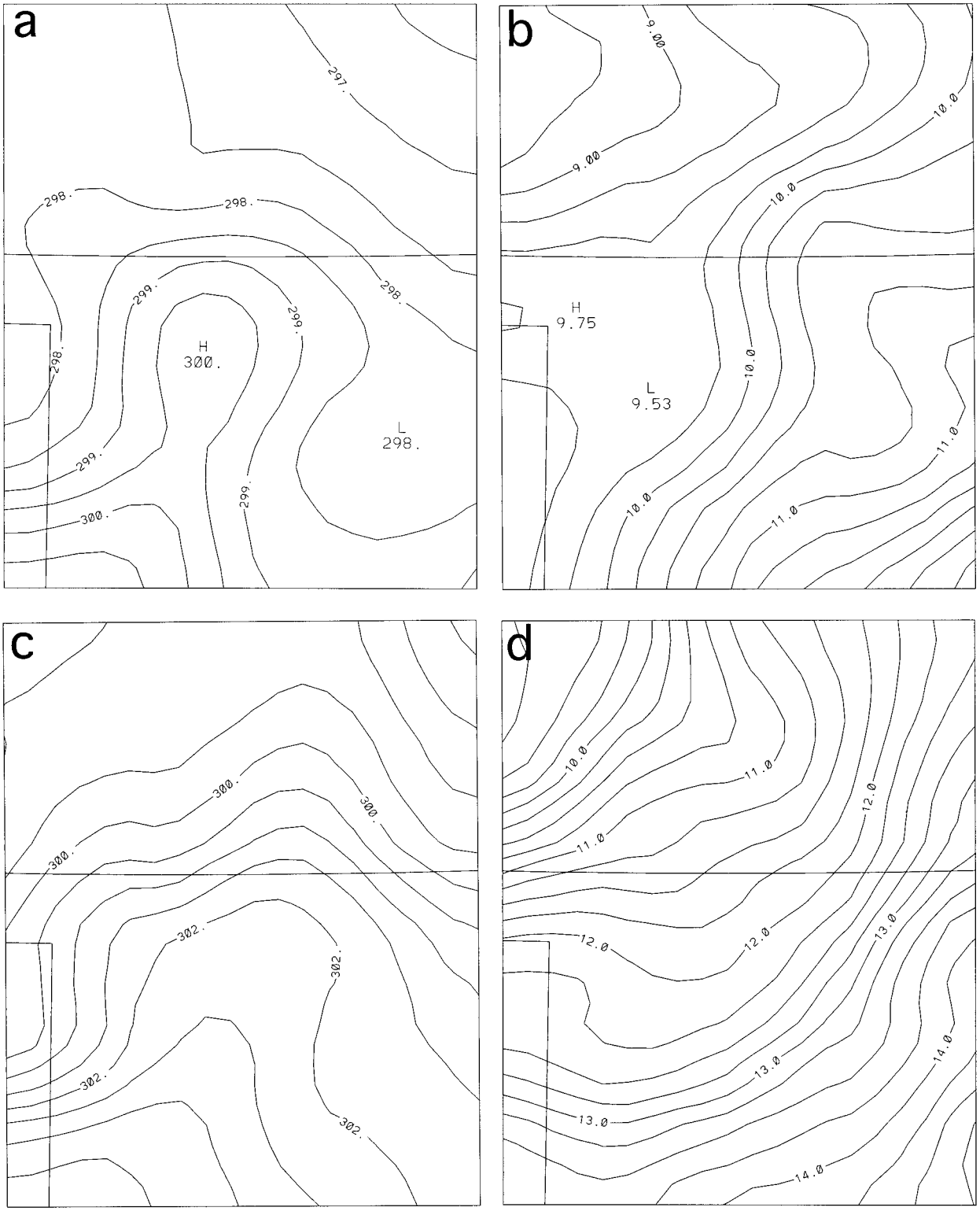

FIG. 2. Objective analysis of the monthly mean values of temperature (K) during (a) May and (c) June at 2100 UTC, and specific humidity (g kg^{-1}) during (b) May and (d) June at 2100 UTC from the mesonetwork stations.

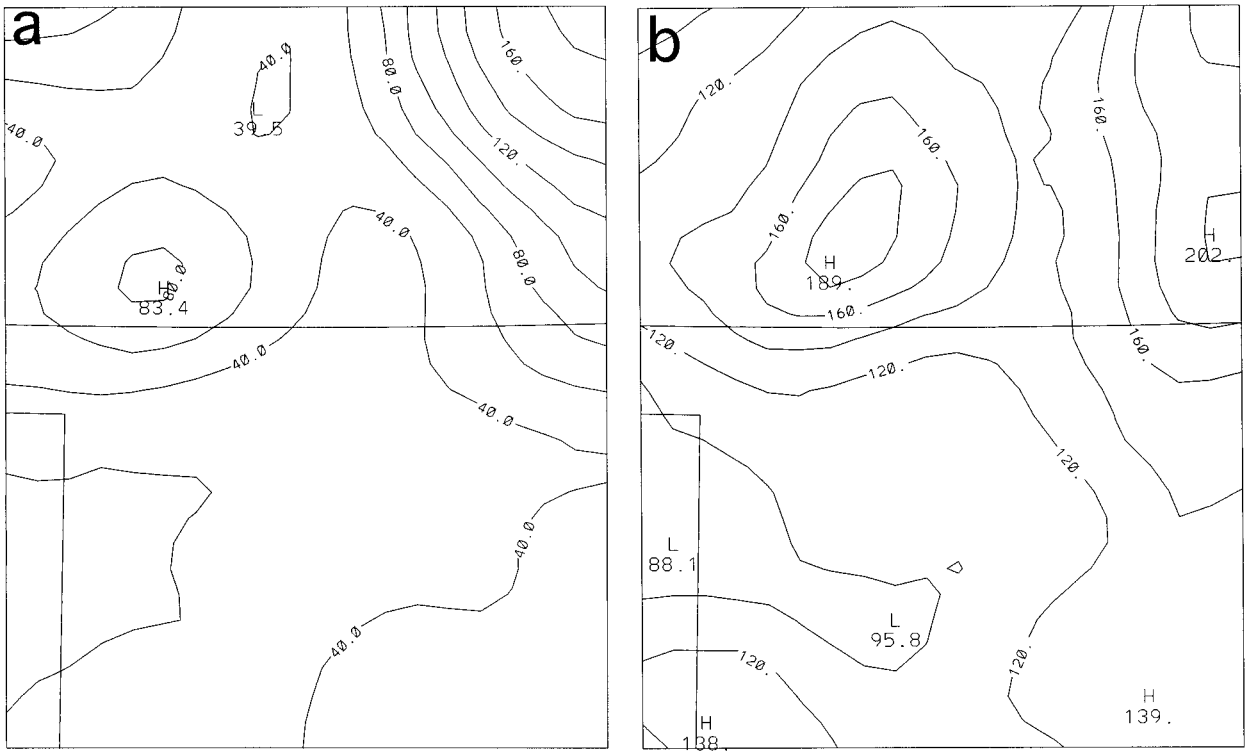

FIG. 3. Objective analysis of the total monthly rainfall (mm) during (a) May and (b) June 1985 from the mesonetwork stations.

Once the monthly mean diurnal cycles of T and q are calculated, the height of the lifting condensation level (LCL) can be calculated at each hour of the day (Bolton 1980, Fig. 6). The maximum values of the LCL height, calculated from the mean diurnal cycle data, for both May and June show that a zone of higher LCL heights stretches from southwestern Oklahoma northward into central Kansas coincident with the T ridge (Figs. 2a,c). Since the mean monthly low-level winds during May and June are southerly to southeasterly at the surface, veering to southerly to southwesterly at 850 hPa according to the National Centers for Environmental Protection (NCEP)–NCAR reanalysis data (Kalnay et al. 1996), the higher LCL heights could be expected to be shifted slightly downwind of the region of winter wheat owing to the horizontal fluxes of heat and moisture.

Calculation of the monthly average surface winds at hourly intervals indicates convergence over this region of winter wheat during the daytime hours (not shown) when the winds are generally southerly (prior to the attainment of the maximum LCL value). This persistent low-level convergence should lead to a deeper PBL and more entrainment of warmer and drier air from the free atmosphere as suggested by the simple mixed layer models of Carson (1973) and Stensrud (1993). This process helps to explain the higher T values and the lower q values. The convergence may be an indication of a mesoscale thermal circulation that develops in response to the strong temperature gradient between the region of wheat stubble (after harvesting) and the surrounding rangeland (Mahfouf et al. 1987; Segal et al. 1988). Further information on processes important to the diurnal surface layer cycles can be ascertained by using conserved variable diagrams.

4. Diurnal cycle classification

The monthly mean diurnal cycles of θ and q can be examined on a conserved variable diagram to evaluate the various processes that contribute to the diurnal cycle (Betts 1982). A summary of the changes to surface layer θ and q produced by various processes are shown in Fig. 7, in which $\boldsymbol{\beta}_{\text{sfc}}$ and $\boldsymbol{\beta}_{\text{inv}}$ denote the surface and inversion-level flux vectors, respectively. Starting at point A, we see that surface sensible and latent heat fluxes tend to warm and moisten the surface layer, while the fluxes owing to entrainment from the inversion at the top of the PBL tend to warm and dry the surface layer. Radiational cooling decreases θ but does not change the value of q. In contrast, both the evaporation of precipitation and the formation of dew (or fog) change both θ and q. Evaporation of precipitation lowers θ and increases q, while maintaining a constant value for θ_e (Betts 1984). The formation of dew or fog lowers both θ and q, while maintaining a constant value of p^*. Therefore, it is possible to determine the most important processes that drive the evolution of the surface layer by examining the evolution of the diurnal cycle.

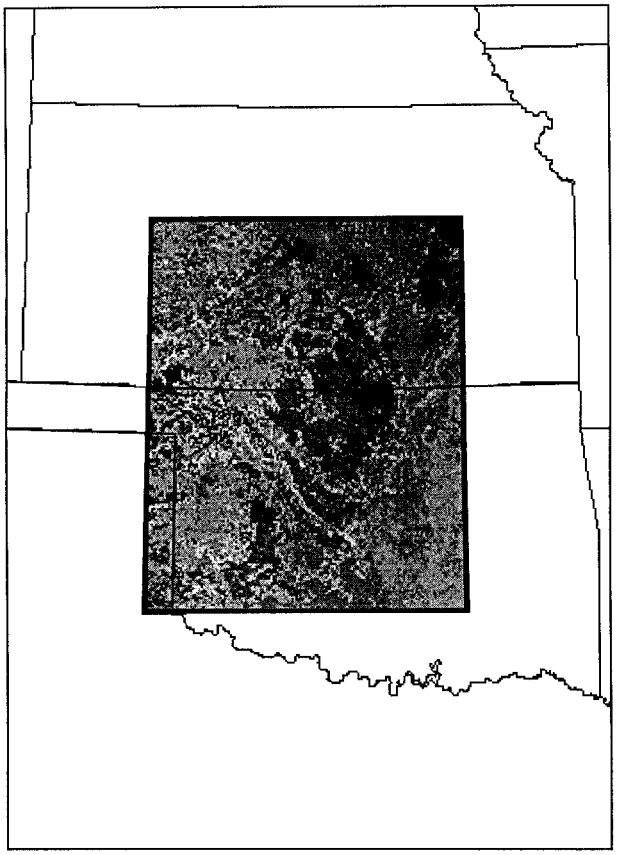

FIG. 4. Depiction of the different vegetation types over Kansas and Oklahoma with the PRE-STORM domain outlined. Areas of winter wheat are indicated by the darkest shading and stretch from southwest Oklahoma into southcentral Kansas.

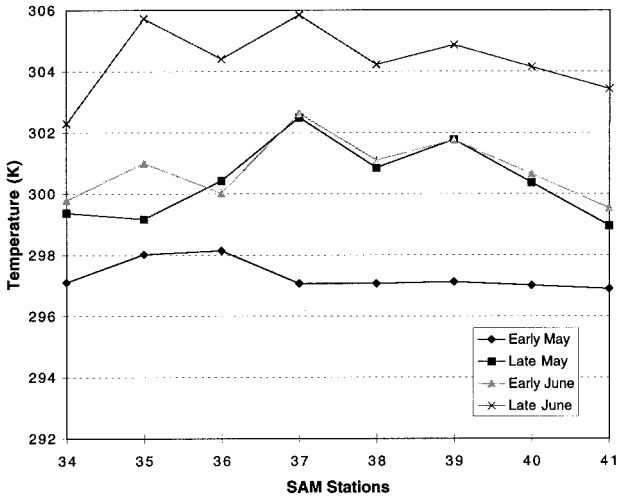

FIG. 5. West to east cross section of the mean 2100 UTC temperature (K) through the PRE-STORM domain from SAM34 to SAM41 (see Fig. 1) during early and late May and June. The ''early'' portion of the month are mean values of the mesonetwork temperatures during the first 15 days of the month, whereas the ''late'' portion of the month are mean values during the remaining days of either May or June.

The effects of advection are the most difficult to account for properly. Betts and Ball (1994) use longer time averages to reduce the advective component of the PBL budget. Unfortunately, by calculating only a monthly average, the effects of advection cannot be removed entirely. Monthly averages of both the winds and the specific humidities are calculated for each hour of the day and used to estimate the magnitude and sign of the advective effects. Results indicate that advection in general produces an increase in q over the entire region at each hour of the day, since the mean winds are southerly across most of the domain and values of q typically decrease from southeast to northwest. There are times where advection of q is negative, but this occurs only for 25 of the 84 mesonet stations over at most a continuous 7-h period. The maximum value of advection calculated from these mean fields is 0.3 g kg^{-1} h^{-1} and occurs during June in the southwestern portion of the domain, while the minimum value of advection is calculated to be -0.15 g kg^{-1} h^{-1} and occurs during May in the east-central portion of the domain. Therefore, unless stated otherwise, it is assumed that advective effects in the mean produce an increase in the values of q.

A subjective examination of the diurnal cycles of each mesonet station using both May and June monthly average data indicates that there are four general types of diurnal cycles (Fig. 8). While no two diurnal cycles are exactly alike, many show similarities in the general evolution of the surface layer. The separation into four types is based upon the dominant physical processes that are suggested in these diurnal cycles. Each type of diurnal cycle is discussed below.

a. Type I

The first type of diurnal cycle shows very little variation in the values of q throughout the day (Fig. 8a), indicating a balance between moistening from surface latent heat flux and drying from entrainment. Stations with this type of diurnal cycle are only found during June in the northwestern portion of the domain (Fig. 9b), and are associated with the lowest p^* values, indicative of the highest LCLs (Fig. 6b). This is due to the strong effects of entrainment at these stations that offsets the moistening of the PBL from surface latent heat flux, and also possibly from small-surface latent heat flux values. The evolution of θ shows the diurnal heating cycle with warming occurring after 1200 UTC and radiational cooling after 2100 UTC. Slight drying is indicated consistently between 1500 and 2200 UTC, likely owing to entrainment of drier air from the top of the PBL, but it amounts to less than a 1 g kg^{-1} change in specific humidity during the daytime. Early in the evening, from 2300 to 0100 UTC, the temperatures drop

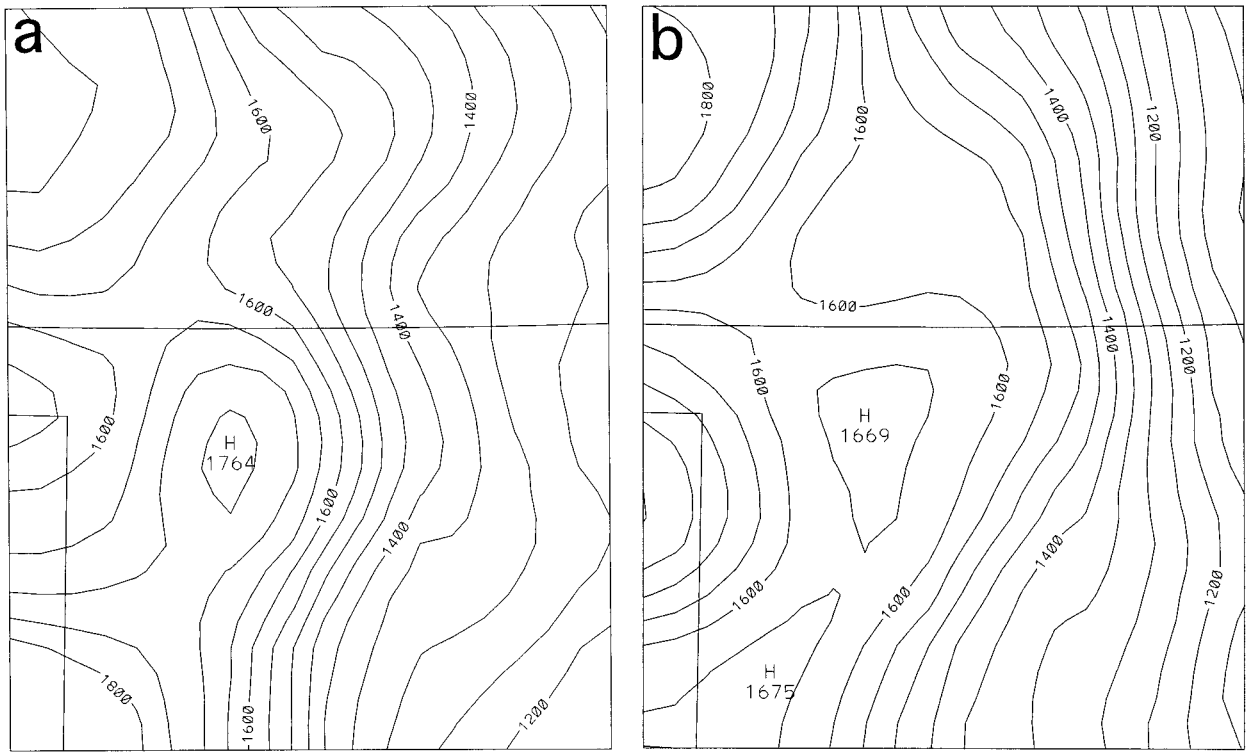

FIG. 6. Maximum monthly mean heights (m) of the lifting condensation level during (a) May and (b) June 1985 calculated from the mean diurnal cycles of surface mesonetwork sites.

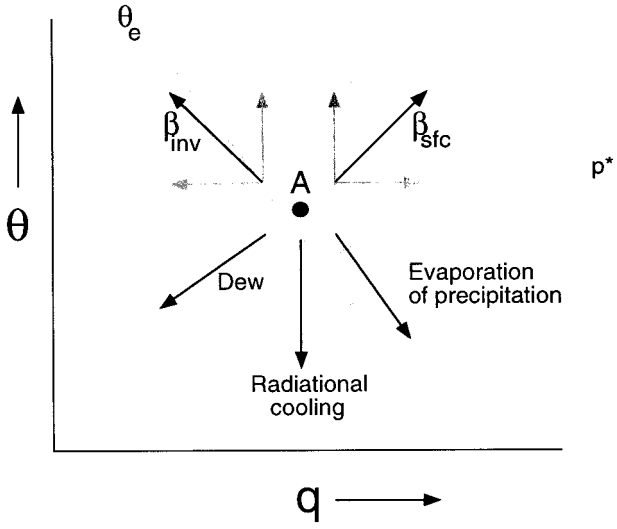

FIG. 7. Idealized depiction of the direction various physical processes will move parcel A on a conserved variable diagram, where θ is potential temperature (K) and q is specific humidity (g/kg), and $\boldsymbol{\beta}$ is the surface flux vector. Black arrows denote the directions that the physical processes will move parcel A, while gray arrows denote the most extreme values that could be taken by the surface flux vector $\boldsymbol{\beta}$. Lines of constant equivalent potential temperature (θ_e) and constant saturation pressure (p^*) are noted.

but moistening continues, indicative of continued transpiration after the surface layer has decoupled from the rest of the PBL. After 0100 UTC the values of θ continue to decrease owing to radiational cooling, while the values of q remain nearly constant. Thus, over this 1-month time period the moistening effects of evapotranspiration from the ground surface and horizontal advection are just balanced by entrainment drying. This diurnal cycle is found in the only area of the PRESTORM domain where the soil moisture is considered very dry (NOAA 1985).

b. Type II

The second general type of diurnal cycle resembles a titled ellipse on a θ–q diagram (Fig. 8b). The PBL both moistens and warms throughout the daytime (1200–2200 UTC), suggesting that surface latent heat fluxes are large enough to overwhelm the entrainment of drier air that occurs at the top of the PBL. Stations with this type of diurnal cycle occur in the northwestern portion of the domain during May (Fig. 9a) and in the northeastern and southwestern part of the domain during June (Fig. 9b). Note that a number of the type II cycles during May become type I diurnal cycles during June, which is suggestive of a reduced latent heat flux during June, possibly owing to senescence of the vegetation, and drier air being entrained from above the PBL. Hor-

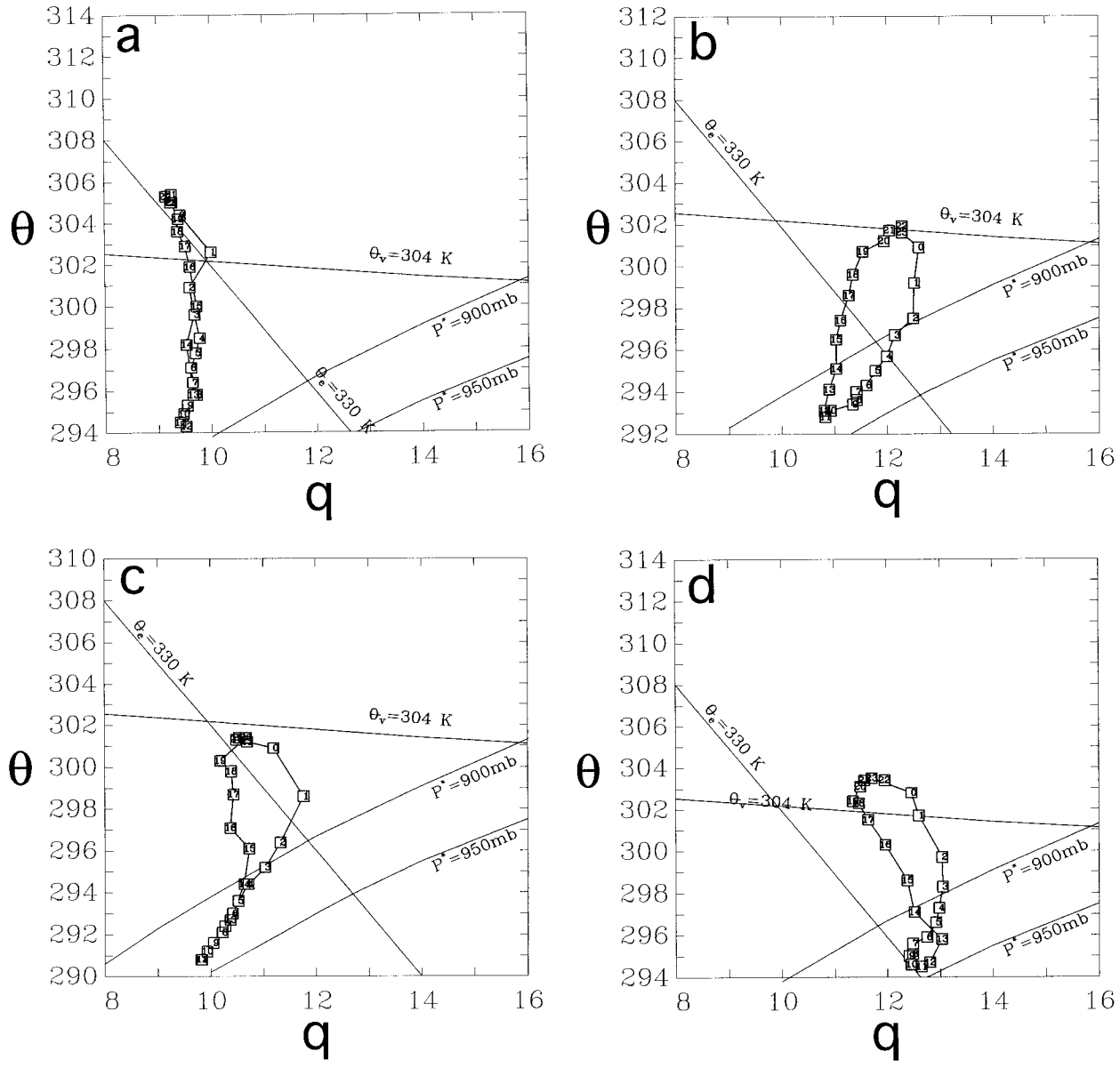

FIG. 8. Monthly mean diurnal cycles of θ (K) and q (g kg^{-1}) from various surface mesonetwork stations illustrating the (a) type I (SAM18—June), (b) type II (PAM 7—June), (c) type III (PAM29—May), and (d) type IV (PAM30—June) diurnal cycles. Lines of constant saturation pressure (p*), equivalent potential temperature (θ_e), and virtual potential temperature (θ_v) are noted. Numbers on the diurnal cycles indicate the time in UTC of the mean observation.

izontal advection also is important. Stations with this type of diurnal cycle are located in regions with north–south gradients in q and larger surface mean wind speeds (not shown). Therefore, the positive advection of q, combined with surface latent heat flux, is able to overcome the drying effects of entrainment.

In the mean diurnal cycle, the surface cools rapidly between 0000 and 0200 UTC, while the mean values of q remain constant, indicative of radiational cooling. After 0200 UTC the surface both cools and dries, with the mean value of q decreasing by almost 2 g kg^{-1}. While mean advective effects decrease q at this site after 0800 UTC, the mean advection cannot account for the magnitude of the decrease in q. Therefore, the decrease in both θ and q illustrates the continuing effects of radiational cooling and both the episodic mechanical mixing of this low-level air with drier air from the residual layer and the formation of dew and fog. Monteith (1957) shows that dew formation can occur within just a few hours after sunset with maximum rates of dewfall found to be 35 g m^{-2} h^{-1}. Dew fall and fog can account for the decrease in q of several g kg^{-1} during the nighttime, as shown in the diurnal cycle from 15 June (Fig. 10), where the formation of dew is indicated between 0600

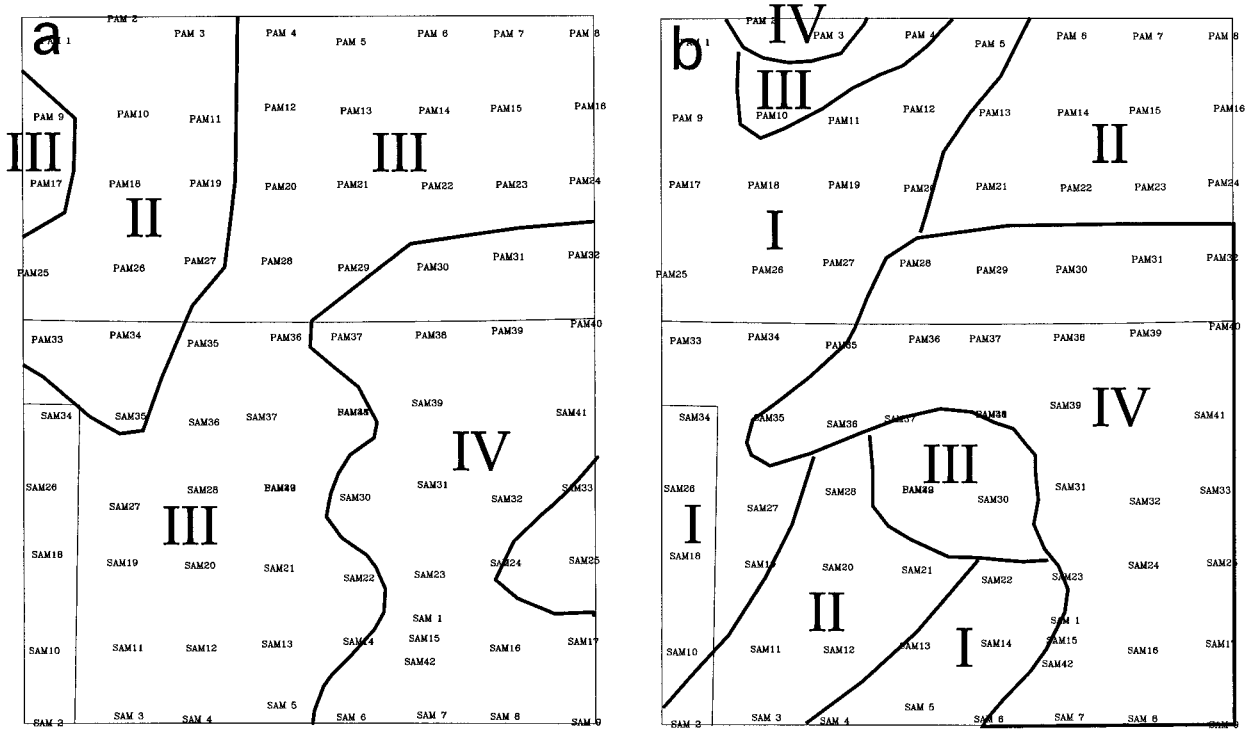

FIG. 9. Horizontal plot of the PRE-STORM domain showing the subjectively determined regions of the four types of diurnal cycles for (a) May and (b) June 1985.

and 1100 UTC by the slope of the diurnal cycle lying parallel to lines of constant p^* (station pressure ~960 hPa). The values of q decrease from 9.5 to 6.4 g kg^{-1} during this time period.

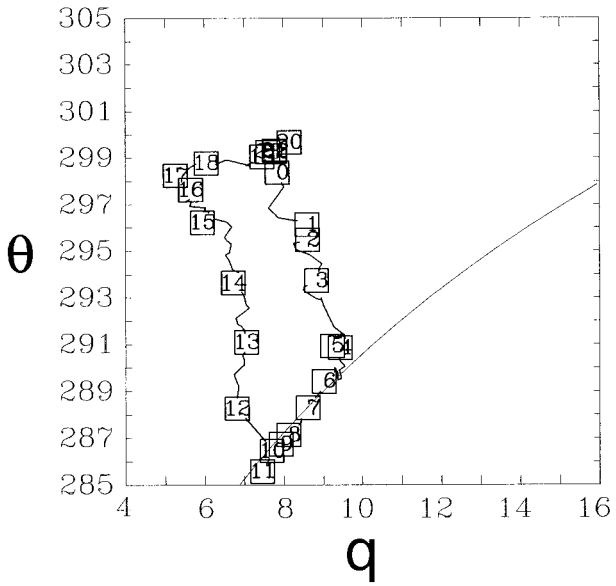

FIG. 10. Diurnal cycle of θ (K) and q (g kg^{-1}) from station PAM 7 beginning 1200 UTC 15 June 1985. Lines of constant p^* are indicated by the curved lines. Numbers indicate the time in UTC of the observation. Data are plotted every 5 min.

c. *Type III*

The third type of diurnal cycle is very similar to type II, except that there is a transition from moistening to slight drying in the surface layer during the late morning (Fig. 8c). Stations with this type of diurnal cycle are most prevalent during May, where half of the stations have this behavior, while only a handful of stations in June are type III (Fig. 9). These stations also have a similarity in that the θ and q lines overlap during the morning segments of the diurnal cycle between 0500 and 1300 UTC (Fig. 8c). Even though the slopes of the θ and q lines are not parallel to the lines of constant p^*, an indication of condensation, the overlapping values of θ and q suggests that dew and fog formation is still a frequent occurrence. Examination of the daily diurnal cycles from this station supports this conclusion, with dew formation indicated clearly on 13 of the 31 days of data. In addition, the morning LCL heights are lowest for this diurnal cycle than any of the others, indicating that the surface layer in the mean is much closer to saturation. After 1300 UTC the dew is completely evaporated and the PBL deepens more rapidly. Entrainment drying begins to offset the surface moistening from evaporation and positive horizontal moisture advection after 1500 UTC as indicated by the small decrease in q with time. As with the other diurnal cycles, evaporation continues after the maximum heating is observed at 2300 UTC, causing q to increase by 0.5 g

kg^{-1} in 1 h. Continued residual evaporation persists until 0100 UTC, after which time q begins to decrease owing to the formation of dew and fog.

d. Type IV

The last general type of diurnal cycle discerned in the dataset has a very different shape that resembles a tilted figure eight (Fig. 8d). Similar to the type III cycle, q initially increases in the early morning from 1100 to 1300 UTC while θ is also increasing, but this initial increase is followed by an abrupt and continual decrease in q after 1300 UTC. The decrease in q occurs earlier and is more rapid than that found in the type III diurnal cycle (Fig. 8c). This indicates that the entrainment drying is the dominant process influencing the PBL and occurs earlier for this diurnal cycle than any other. Latent heat fluxes continue after the maximum heating is observed at 2300 UTC, causing q to increase late in the day until 0200 UTC. Values of θ then begin to decrease, suggestive of radiational cooling, but the values of q also decrease with a rapid decrease of 0.5 g kg^{-1} between 0500 and 0700 UTC. After 0700 UTC, θ decreases while q remains constant, which is again suggestive of radiational cooling. Stations with this type of diurnal cycle are found in both May and June. During May this type of cycle is found in the easternmost portion of the domain (Fig. 9a), whereas in June this type of cycle is found stretching southwest to northeast across the central portion of the domain, and also along the southeastern boundary (Fig. 9b).

The main difference between this diurnal cycle and that of type III is the early and rapid decrease of q in the morning hours and the cooling and drying that occurs between 0200 and 0700 UTC at pressures greater than p^*, as indicated by the continued radiational cooling that occurs after 0700 UTC. In the mean, the drying that occurs between 0200 and 0700 UTC occurs above saturation. Some process other than dew and fog formation is decreasing the values of q in the surface layer during the early morning hours.

Examination of the daily diurnal cycle data suggests that one process that could produce this evolution of the diurnal cycle, causing the surface layer to both cool and dry before reaching saturation, is convection. During the months of May and June 1985, numerous mesoscale convective complexes (MCCs) and mesoscale convective systems (MCSs) passed across the PRE-STORM mesonetwork (Augustine and Howard 1988). A composite image of the frequency of satellite observed infrared temperatures of less than -38°C shows that deep convection was a common occurrence during these two months (Fig. 11). The zone of higher frequencies stretching from the Texas panhandle northeastward into Missouri shows the preferred track of the MCSs for June (Fig. 11b). This track is through the center of the PRE-STORM surface mesonetwork and over the location of the station used to illustrate the type IV diurnal cycle. Since convection over the southern plains is most frequent during the nighttime hours (Wallace 1975), the effects of convective activity on a monthly average diurnal cycle might be most apparent between 0000 and 1200 UTC.

A conserved variable plot from 1200 UTC 21 June through 1200 UTC 22 June shows significant cooling and drying occurs between 0200 and 0300 UTC on 22 June (Fig. 12). This dramatic change in surface layer values is produced by the passage of a convective line over the mesonetwork station and the replacement of preconvective boundary layer air with downdraft air. Between 0300 and 0600 the diurnal cycle follows a line of constant θ_e with θ decreasing and q increasing. This evolution is suggestive of the evaporation of rain (Betts 1984) in the stratiform region of an MCS that follows the passage of the gust front. Similar examples of the changes in air mass are seen in the horizontal plots across the mesonetwork in Johnson and Hamilton (1988) from the 10–11 June squall line. To identify signals of downdrafts in the surface data, the hourly data are searched for the number of times that q decreases by 1.5 g kg^{-1} and θ decreases by 2.5°C during a 1-h time period between 0000 and 1200 UTC. These events should indicate the passage of strong convective lines over the surface stations during the morning hours, although it may also be associated with the formation of dew and fog at sites that are in a drier atmosphere that cool more quickly. These results are then objectively analyzed and overlaid with the horizontal distribution of the type IV diurnal cycles and the region with cold cloud-top frequencies of more than 15% (Fig. 13). There is a local maximum along the western portion of the domain, which is suggestive of rapid radiational cooling in the drier portion of the domain (Figs. 2b,d). However, there is also a local maximum in the eastern portion of the domain during May (Fig. 12a) and in the central portion of the domain during June (Fig. 12b). Both of these regions are collocated with regions of cold cloud-top frequencies of more than 15% (see Fig. 11). Therefore, during both May and June there is a consistent relationship between the regions with frequent cold cloud tops, a higher number of strong convective line passages, and the locations of the type IV diurnal cycles.

The hourly mesonetwork data also can be subdivided into days with and without convection to illustrate the different diurnal cycles of wet and dry days (Betts 1992). If we average all the stations during May with rainfall greater than 2 cm between 0000 and 1200 UTC (a total of 45 stations), characteristic of heavy convection during the nighttime hours, the resultant diurnal cycle is very similar to the type IV diurnal cycle (Fig. 14a). In contrast, the diurnal cycle for the dry days is similar to a type III diurnal cycle (Fig. 14b).

One possible explanation for the rapid decrease in q after 1300 UTC is also related to convection. Mesoscale convective systems often produce onion-type soundings (Zipser 1977) along their back edge. These onion-type

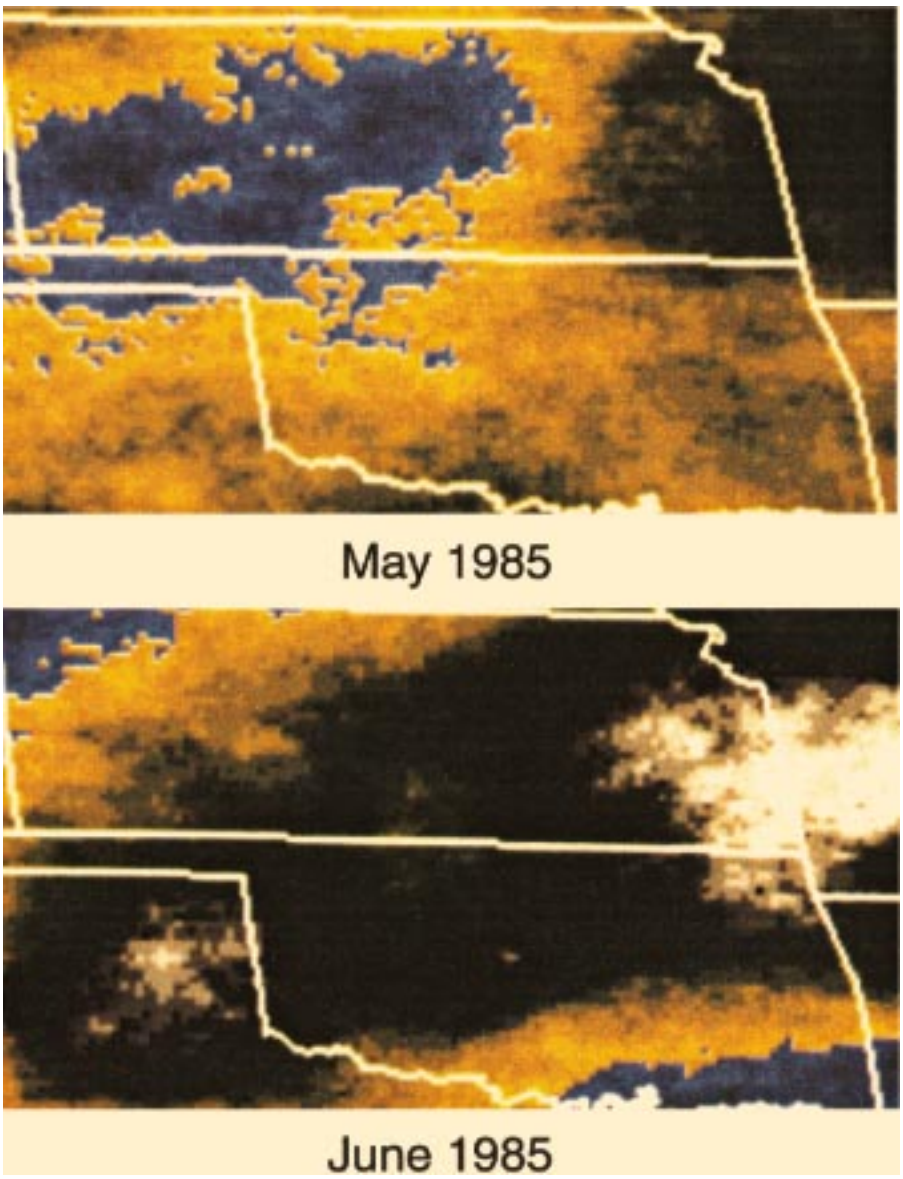

FIG. 11. Frequency of satellite observed infrared temperatures of less than −38°C during May and June 1985 as determined from hourly data. Colors from dark blue to light blue indicate frequencies of 5%–10%, yellow to black indicates frequencies of 10%–20%, and black to white indicates frequencies of 20%–25%.

soundings are typified by a shallow layer of moist air near the surface with a deeper layer of much drier air just above the surface. After a nocturnal MCS produces this type of low-level atmospheric structure, the effects of solar heating would initially warm and moisten the shallow PBL until the overlying dry layer begins to be entrained. At this point, the entire PBL begins to dry rapidly. This behavior is consistent with the type IV diurnal cycle, although there is a lack of sufficient upper-air data to verify this hypothesis. Nonetheless, the results presented herein strongly suggest that convective downdrafts help produce the type IV diurnal cycle during both May and June, and that downdrafts contribute substantially to the observed monthly mean diurnal cycles of the surface layer.

A subjective evaluation of the horizontal placement of the four categories of diurnal cycles suggests that these are closely tied to both vegetation and convection. Vegetation in general changes from east to west, but with a southwest–northeast orientation (Fig. 4). This is very similar to the general orientation of the diurnal cycle types during May (cf. Figs. 4 and 9a). The same is true for June (Fig. 9b), except that the type IV diurnal cycles interrupt the general east to west progression of the different types. The type IV diurnal cycle follows the main track of the MCSs as suggested by the highest

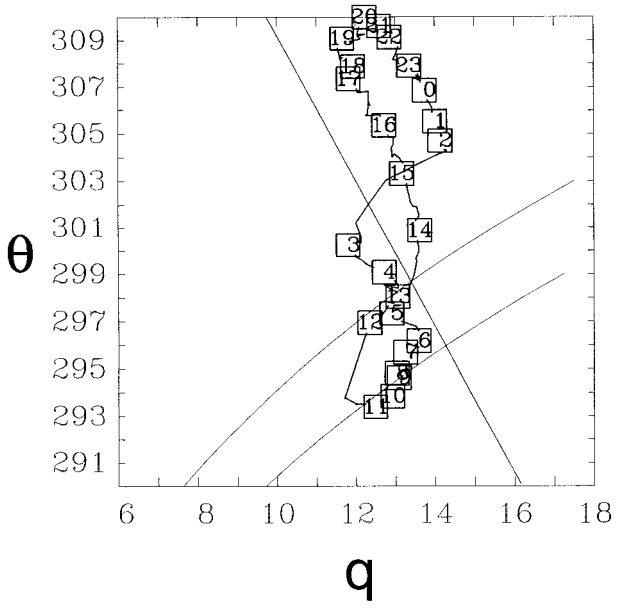

FIG. 12. Diurnal cycle of θ (K) and q (g kg^{-1}) from station PAM30 beginning 1200 UTC 21 June 1985. Lines of constant p^* are indicated by the curved lines. Numbers indicate the time in UTC of the observation. Data are plotted every 5 min for a 24-h time period.

frequencies of cold cloud tops near the Oklahoma–Kansas border (Fig. 11). The influence of these diurnal cycles on the calculation of surface Bowen ratios is now examined within the context of tuning model surface parameterizations from observations.

5. Surface Bowen ratios

Betts and Ball (1995) indicate that the early morning evolution of θ and q are related to the observed surface Bowen ratio and soil moisture. Their results show that the smaller the slope ($d\theta/dq$), the lower the surface Bowen ratio (β) and the larger the soil moisture. While there are no measurements of surface fluxes available during the PRE-STORM experiment, the results of Betts and Ball (1995) suggest that it is possible to estimate the relative magnitude of the surface fluxes from the monthly mean diurnal cycles using the early morning slope ($d\theta/dq$) values. The mean diurnal cycle data between 1100 and 1500 UTC from each station during both May and June are used to calculate estimates of β. If the values of β from May are subtracted from the June values, the difference in β should be positive if the soil is drier in June than in May. Results from this difference calculation suggest that the soil is drier in June than in May (Fig. 15) across the region where numerous MCSs occurred during June (Fig. 11). Yet observations indicate that rainfall in excess of 10 cm fell across much

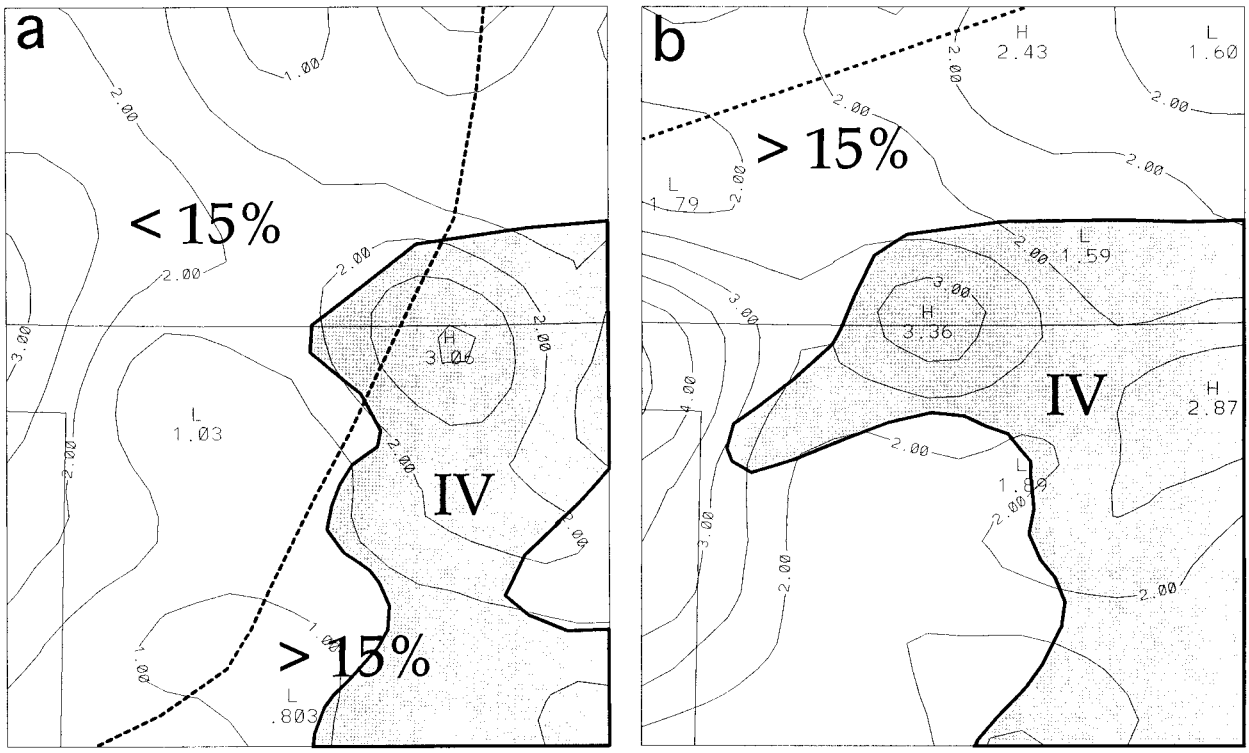

FIG. 13. Objective analysis of the number of strong cooling and drying events between 0000 and 1200 UTC observed by the mesonetwork stations overlaid with the line of 15% frequency of cold cloud-top temperatures and the region of the type IV diurnal cycles during (a) May and (b) June 1985.

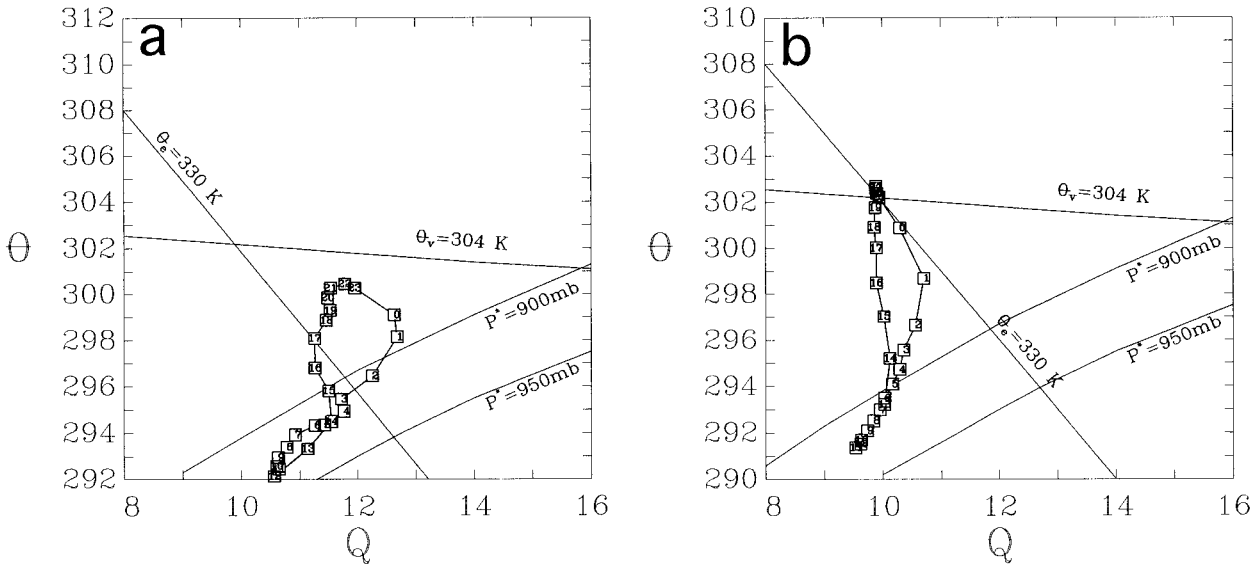

FIG. 14. Mean diurnal cycles of θ (K) and q (g kg^{-1}) from (a) stations during May with rainfall of 2 cm or greater between 0000 and 1200 UTC, and (b) stations with no rainfall during May. Numbers indicate the time in UTC of the observation. Data are plotted every 5 min for a 24-h time period.

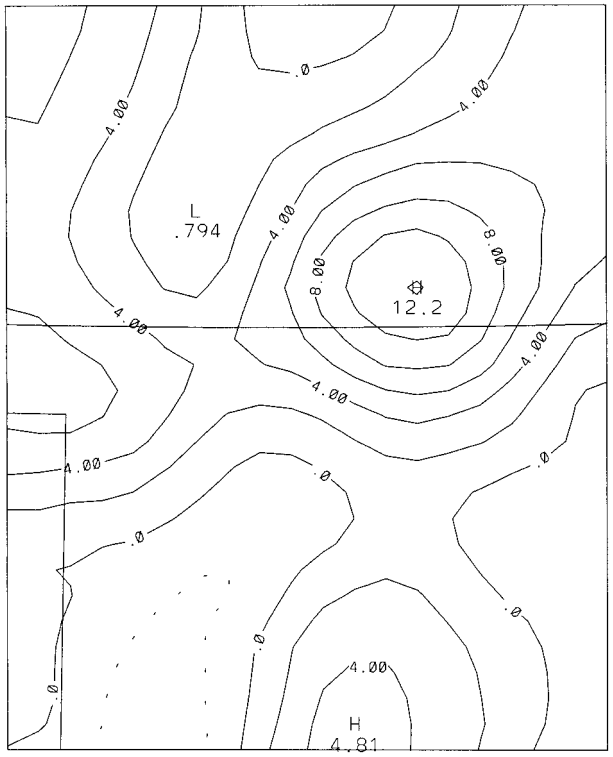

FIG. 15. Objective analysis of the differences in the mean 1200–1600 UTC Bowen ratio angles (proportional to $\beta L_v/c_p$, where L_v is the latent heat of vaporization and c_p is the specific heat at constant pressure) between June and May 1985. The Bowen ratio angle refers to the slope a given value of the Bowen ratio would have on a θ–q diagram, such that a 0° angle is horizontal and a 90° angle is vertical, indicating Bowen ratios of zero and infinity, respectively. For this figure, positive values indicate that the June surface layer is warming and drying faster than the May surface layer during this time period.

of Oklahoma and Kansas during June, suggesting that the soil should be fairly moist. Indeed, soil moisture in June was considered abnormally moist (NOAA 1985). These observations are in direct conflict with the larger estimated Bowen ratio during June. The answer to this apparent paradox is that the effects of convection in the type IV diurnal cycles contaminate the calculations, since for these cycles the entrainment drying occurs very early in the day and yields a large value for β. Therefore, it is possible to make an incorrect interpretation of the partitioning of surface heat fluxes using only the surface station data, since averaging days with and without rainfall can lead to difficulties in interpretation.

This problem with the analysis of surface data is an important one to consider, since Sellers and Hall (1992) suggest that one may be able to tune soil moisture in general circulation models by finding the value of soil moisture that replicates the observed surface time series of temperature and humidity. However, in regions where convective downdrafts are frequent, producing a type IV diurnal cycle, this type of analysis would likely determine that June is drier than May, when the reverse is true. As argued by Betts et al. (1994), it is possible to reproduce the time series of surface observations and have both the wrong surface fluxes and soil moisture values. This analysis provides an example of the difficulties with estimating soil moisture from time series of surface observations.

6. Discussion

Data from 84 surface mesonetwork stations have been used to calculate monthly mean diurnal cycles during

May and June of 1985. The horizontal variations across the mesonetwork domain are large, even though this domain is only 350 km × 450 km large. Landscape differences appear to have caused much of this variation, with the harvesting of winter wheat over a large region of Oklahoma in late May being one of the more clear factors influencing the surface layer cycles. A subjective classification of the mean monthly diurnal cycles shows that the type of diurnal cycle changes as the vegetation changes.

The mean diurnal cycles also show clearly the effects of convective downdrafts, indicating that the interaction of convection with the atmospheric surface layer is an important process even on monthly timescales. This is important to consider for those trying to produce regional climate simulations over various parts of the globe. Not all convective parameterization schemes include the effects of convective downdrafts (Emanuel and Raymond 1993), indicating that the diurnal cycles produced by some regional climate models may not replicate the observations. When comparing model output with observations, one must be concerned with how convection is represented in both the *model and observations* in order to understand fully which evolution in the mean diurnal cycles can be replicated by the model and which cannot be replicated. Otherwise, this comparison could lead to an incorrect conclusion and an improper change in the model physical parameterizations for surface processes.

Acknowledgments. This work was largely accomplished when the first author (PMM) was in the Research Experience for Undergraduates at the Oklahoma Weather Center during the summer of 1995. Major funding for the REU program was provided by the National Science Foundation under Grant ATM 9424209. Additional funding was provided by the NSSL, the Center for the Analysis and Prediction of Storms, the Cooperative Institute for Mesoscale Meteorological Studies, and the School of Meteorology at the University of Oklahoma. Additional information about this REU program can be found in Cortinas et al. (1996). Discussions with Dr. Jeanne Schneider were very helpful. We also appreciate the constructive and helpful reviews from Dr. Conrad Ziegler and two anonymous reviewers who greatly improved this presentation.

REFERENCES

Anthes, R. A., 1984: Enhancement of convective precipatation by mesoscale variations in vegetative covering in semiarid regions. *J. Climate Appl. Meteor.*, **23,** 541–554.

Augustine, J. A., and K. W. Howard, 1988: Mesoscale convective complexes over the United States during 1985. *Mon. Wea. Rev.*, **116,** 685–701.

Avissar, R., and Y. Liu, 1996: Three-dimensional numerical study of shallow convective clouds and precipitation induced by land surface forcing. *J. Geophys. Res.*, **101,** 7499–7518.

Benjamin, S. G., and T. N. Carlson, 1986: Some effects of surface heating and topography on the regional severe storm environment. Part I: Three-dimensional simulation. *Mon. Wea. Rev.*, **114,** 307–329.

Betts, A. K., 1973: Non-precipitation cumulus convection and its parameterization. *Quart. J. Roy. Meteor. Soc.*, **99,** 178–196.

——, 1975: Parametric interpretation of trade-wind cumulus budget studies. *J. Atmos. Sci.*, **32,** 1934–1945.

——, 1982: Saturation point analyses of moist convective overturning. *J. Atmos. Sci.*, **39,** 1484–1505.

——, 1984: Boundary layer thermodynamics of a High Plains severe storm. *Mon. Wea. Rev.*, **112,** 2199–2211.

——, 1985: Mixing line analysis of clouds and cloudy boundary layers. *J. Atmos. Sci.*, **42,** 2751–2763.

——, 1992: FIFE atmospheric boundary layer budget methods. *J. Geophys. Res.*, **97,** 18 523–18 531.

——, and J. H. Ball, 1994: Budget analysis of FIFE-1987 sonde data. *J. Geophys. Res.*, **99,** 3655–3666.

——, and ——, 1995: The FIFE surface diurnal cycle climate. *J. Geophys. Res.*, **100,** 25 679–25 693.

——, R. L. Desjardins, and J. I. MacPherson, 1992: Budget analysis of the boundary layer grid flights during FIFE 1987. *J. Geophys. Res.*, **97,** 18 533–18 546.

——, ——, and A. C. M. Beljaars, 1993: Comparison between the land surface response of the European Centre model and the FIFE-1987 data. *Quart. J. Roy. Meteor. Soc.*, **119,** 975–1001.

——, ——, ——, M. J. Miller, and P. Viterbo, 1994: Coupling between land surface, boundary layer parameterizations and rainfall on local and regional scales: Lessons from the wet summer of 1993. Preprints, *Fifth Symp. on Global Change Studies*, Nashville, TN, Amer. Meteor. Soc., 174–181.

Bolton, D., 1980: The computation of equivalent potential temperature. *Mon. Wea. Rev.*, **108,** 1046–1053.

Carlson, T. N., and F. H. Ludlam, 1968: Conditions for the formation of severe local storms. *Tellus*, **20,** 203–226.

——, R. A. Anthes, M. N. Schwartz, S. G. Benjamin, and D. G. Baldwin, 1980: Analysis and prediction of severe storms environment. *Bull. Amer. Meteor. Soc.*, **61,** 1018–1032.

——, S. G. Benjamin, G. S. Forbes, and Y.-F. Li, 1983: Elevated mixed layers in the severe-storm environment—Conceptual model and case studies. *Mon. Wea. Rev.*, **111,** 1453–1473.

Carson, D. J., 1973: The development of a dry inversion-capped convectively unstable boundary layer. *Quart. J. Roy. Meteor. Soc.*, **99,** 450–467.

Chang, J.-T., and P. J. Wetzel, 1991: Effects of spatial variations of soil moisture and vegetation on the evolution of a pre-storm environment: A numerical case study. *Mon. Wea. Rev.*, **119,** 1368–1390.

Cortinas, J. V., Jr., J. M. Straka, W. H. Beasley, J. M. Schneider, and C. M. Machacek, 1996: The research experiences for undergraduates program: The 1995 program at the Oklahoma Weather Center. *Bull. Amer. Meteor. Soc.*, **77,** 2925–2936.

Cressman, G. P., 1959: An operative objective analysis scheme. *Mon. Wea. Rev.*, **87,** 367–374.

Cunning, J. B., 1986: The Oklahoma–Kansas preliminary regional experiment for STORM-Central. *Bull. Amer. Meteor. Soc.*, **67,** 1478–1486.

Diak, G., S. Heikkinen, and J. Bates, 1986: The influence of variations in surface treatment on 24-h forecasts with a limited area model, including a comparison of modeled and satellite-measured surface temperatures. *Mon. Wea. Rev.*, **114,** 215–232.

Doswell, C. A., III, F. Caracena, and M. Magnano, 1985: Temporal evolution of 700–500 mb lapse rate as a forecasting tool—A case study. Preprints, *14th Conf. on Severe Local Storms*, Indianapolis, IN, Amer. Meteor. Soc., 398–401.

Emanuel, K. A., and D. J. Raymond, 1993: *The Representation of Cumulus Convection in Numerical Models. Meteor. Monogr.*, No. 46, Amer. Meteor. Soc., 246 pp.

Graziano, T. M., and T. N. Carlson, 1987: A statistical evaluation of lid strength on deep convection. *Wea. Forecasting*, **2,** 127–139.

Johnson, R. H., and P. J. Hamilton, 1988: The relationship of surface

pressure features to the precipitation and airflow structure of an intense midlatitude squall line. *Mon. Wea. Rev.*, **116,** 1444–1472.
Kalnay, E., and Coauthors, 1996: The NCEP/NCAR 40-year reanalysis project. *Bull. Amer. Meteor. Soc.*, **77,** 437–471.
Lakhtakia, M. N., and T. T. Warner, 1987: A real-data numerical study of the development of precipitation along the edge of an elevated mixed layer. *Mon. Wea. Rev.*, **115,** 156–168.
Lanicci, J. M., T. N. Carlson, and T. T. Warner, 1987: Sensitivity of the Great Plains severe-storm environment to soil moisture distribution. *Mon. Wea. Rev.*, **115,** 2660–2673.
Lilly, D. K., 1968: Models of cloud-topped mixed layers under a strong inversion. *Quart. J. Roy. Meteor. Soc.*, **94,** 292–309.
Loveland, T. R., J. W. Merchant, J. F. Brown, D. O. Ohlen, B. C. Reed, P. Olson, and J. Hutchinson, 1995: Seasonal land-cover regions of the United States. *Ann. Assoc. Amer. Geographers*, **85,** 339–355.
Mahfouf, J.-F., E. Richard, and P. Mascart, 1987: The influence of soil and vegetation on the development of mesoscale circulations. *J. Climate Appl. Meteor.*, **26,** 1483–1495.
Monteith, J. L., 1957: Dew. *Quart. J. Roy. Meteor. Soc.*, **83,** 322–341.
NOAA, 1985: *Weekly Weather and Crop Bulletin.* U.S. Dept. of Agriculture, 44 pp.
Ookouchi, Y., M. Segal, R. C. Kessler, and R. A. Pielke, 1984: Evaluation of soil moisture effects on the generation and modification of mesoscale circulations. *Mon. Wea. Rev.*, **112,** 2281–2292.
Rabin, R. M., S. Stadler, P. J. Wetzel, D. J. Stensrud, and M. Gregory, 1990: Observed effects of landscape variability on convective clouds. *Bull. Amer. Meteor. Soc.*, **71,** 272–280.
Rhea, J. O., 1966: A study of thunderstorm formation along drylines. *J. Appl. Meteor.*, **5,** 58–63.
Richman, M. B., and P. J. Lamb, 1985: Climatic pattern analysis of three- and seven-day summer rainfall in the central United States: Some methodological considerations and a regionalization. *J. Climate Appl. Meteor.*, **24,** 1325–1343.
——, and ——, 1987: Pattern analysis of growing season precipitation in southern Canada. *Atmos.–Ocean*, **25,** 137–158.
——, and ——, 1990: Use of cooperative weather station data in contemporary climate research. *Trans. Illinois State Acad. Sci.*, **83,** 70–81.
Segal, M., R. Avissar, M. C. McCumber, and R. A. Pielke, 1988: Evaluation of vegetation effects on the generation and modification of mesoscale circulations. *J. Atmos. Sci.*, **45,** 2268–2292.
——, W. E. Schreiber, G. Kallos, J. R. Garratt, A. Rodi, J. Weaver, and R. A. Pielke, 1989: The impact of crop areas in northeast Colorado on midsummer mesoscale thermal circulations. *Mon. Wea. Rev.*, **117,** 809–825.
Sellers, P. J., and F. G. Hall, 1992: FIFE in 1992: Results, scientific gains, and future research directions. *J. Geophys. Res.*, **97,** 19 091–19 109.
Stensrud, D. J., 1993: Elevated residual layers and their influence on surface boundary layer evolution. *J. Atmos. Sci.*, **50,** 2284–2293.
Wallace, J. M., 1975: Diurnal variations in precipitation and thunderstorm frequency over the conterminous United States. *Mon. Wea. Rev.*, **103,** 406–419.
Ziegler, C. L., W. J. Martin, R. A. Pielke, and R. L. Walko, 1995: A modeling study of the dryline. *J. Atmos. Sci.*, **52,** 263–285.
Zipser, E. J., 1977: Mesoscale and convective-scale downdrafts as distinct components of squall-line circulation. *Mon. Wea. Rev.*, **105,** 1568–1589.